Viscoelastic Modeling of Natural and Synthetic Textile Yarns

A. M. MANICH,[1] P. N. MARINO,[2] M. D. DE CASTELLAR,[1] M. SALDIVIA,[2] R. M. SAURÍ[1]

[1] Ecotechnologies Department, CSIC, Jordi Girona, 18-26, 08034-Barcelona, Spain

[2] Centro de Investigaciones Textiles, INTI, Parque Tecnológico Miguelete, C.C. 157, CP 1650 - San Martín, Buenos Aires, República Argentina

Received 12 May 1999; accepted 10 October 1999

ABSTRACT: Viscoelastic models were employed to analyze the stress–strain behavior of cotton, acrylic, and polyester yarns. The potential model and the modified Maxwell model gave the best fits as regards the stress–strain behavior of these yarns. The results of the potential model resembled those of the modified Maxwell model with an infinite relaxation time. The potential model is suitable for explaining the rearrangement undergone by the yarns when no slippage between fibers under strain occurs. When slippage occurs, Maxwell models are able to explain the stress–strain behavior of the yarns. © 2000 John Wiley & Sons, Inc. J Appl Polym Sci 76: 2062–2067, 2000

Key words: viscoelastic; modeling; yarns; cotton; acrylic; polyester

INTRODUCTION

Viscoelastic modeling has not been widely reported to date owing to the lack of suitable tools. The advent of statistical tools for mathematical modelization of the stress–strain curves has enabled us to reconsider this subject in an attempt to relate the behavior until break with the structure of fibers and yarns. Ward and Hadley[1] and Krausz and Eyring[2] pioneered the application of viscoelastic modelization to fibers and yarns.[3–9] Despite using the methods reported by Vangheluwe[10] and Aksan and Zurek,[11] we sought to simplify the model by introducing a nonlinear element to relate yarn tenacity and yarn strain.

EXPERIMENTAL

Yarns were obtained from 10 fabrics prepared. The characteristics of these yarns are shown in Table I. Tensile tests were carried out on 30 samples of 100 mm randomly selected of each yarn at a speed r of 100 mm/min. As for the viscoelastic modeling, the "strain" X of the samples will be dimensionless (mm/100 mm) and the deformation gradient r will be 100% min^{-1}. During the stress–strain tests, the mean tenacity of the 30 samples F [cN/tex] induced by strain at 0.5, 1, 1.5, 2, 2.5, 3, 3.5, 4, 5, 6, 8%, etc., up to the breaking point in steps of 2% of strain were recorded for viscoelastic modeling employing the models shown below.

Potential Model

This is based on the assumption that yarns are made up of fibers which, owing to their arrangement level during strain according to Hook's law, behave with a nonlinear response. Figure 1 shows the equation which relates the stress F induced in the yarns with deformation X. This corresponds to a spring which offers no resistance to small deformations, but as X increases, the stress also shows an increase. A is the elasticity modulus, and C, the linearity factor of the material. For values of

Correspondence to: M. D. de Castellar.
Contract grant sponsor: Spanish Government.

Journal of Applied Polymer Science, Vol. 76, 2062–2067 (2000)

Table I Yarn Characteristics

Ref.	Composition	Type	Linear Density [tex]	Tenacity [cN/tex]	Break Elongation (%)	Fiber Type
T12	Cotton	Weft	31.5	15.5	6.90	Staple
T13	Polyester	Weft	79.8	24.2	27.8	Filament
T14	Acrylic	Weft	62.9	11.0	33.4	Staple
T15	Polyester	Weft	57.1	26.7	30.0	Filament
T16	Polyester	Weft	41.8	23.2	27.6	Staple
T17	Polyester	Weft	59.1	29.8	35.4	Filament
T18	Polyester	Weft	60.5	21.6	28.0	Filament
T19	Polyester	Weft	77.6	24.6	26.0	Filament
T20	Polyester	Weft	124.5	23.7	29.6	Filament
T21	Acrylic	Weft	64.0	7.96	28.7	Staple
U12	Cotton	Warp	48.8	16.8	14.6	Staple
U13	Polyester	Warp	84.4	22.8	30.7	Filament
U14	Acrylic	Warp	59.7	11.9	35.2	Staple
U15	Polyester	Warp	42.4	25.6	41.3	Staple
U16	Polyester	Warp	41.4	25.4	34.9	Staple
U17	Polyester	Warp	74.4	28.2	36.9	Filament
U18	Polyester	Warp	84.2	25.8	34.7	Staple
U19	Polyester	Warp	77.7	23.7	23.5	Filament
U20	Polyester	Warp	88.3	22.4	28.4	Filament
U21	Acrylic	Warp	60.8	10.9	30.7	Staple

C equal to the unit, the modulus remains constant throughout the deformation process. Values below the unit show that the modulus diminishes with the deformation, the material flows more easily, and, for C values exceeding the unit, the modulus increases with the deformation, becoming firmer and stiffer. The first case shows an arranged structure of fibers which after deformation due to strain begins to slip, whereas the second case shows a disarranged structure which in the early stages of deformation attains high levels of arrangement up to the stress threshold for its components.

Maxwell Model

This model accounts for the permanent deformation phenomena observed in the yarns. According to Figure 2, A is the elastic spring modulus, which is linear with the deformation, and B is the viscosity of the Newtonian piston. The stress-induced by strain X will follow the equation shown

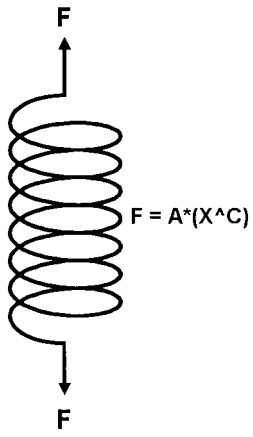

Figure 1 Potential model.

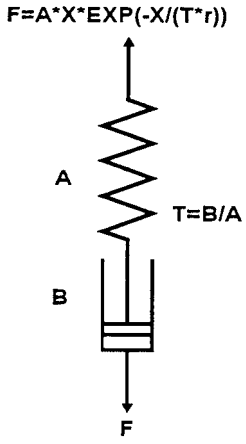

Figure 2 Maxwell model.

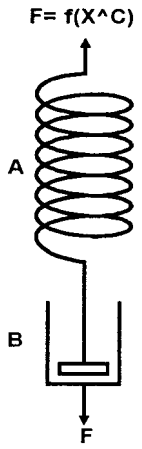

Figure 3 Nonlinear Maxwell model.

in Figure 2. The relaxation time T would be proportional to the slippage speed of the fibers when subjected to a given strain, that is, for very long relaxation times, there would scarcely be any slippage between the fibers and, therefore, the yarn would behave like an elastic solid.

Nonlinear Maxwell Model

The Maxwell model does not fit the behavior of some of the yarns under study. The response of these was nonlinear with respect to deformation. Thus, if the deformation X of the sample is replaced by $(X\text{^}C)$ so that it can be adapted to a nonlinear response, the nonlinear Maxwell model is obtained, as shown in Figure 3.

Model Fitting

Model fitting was made in two steps: First, using the logarithmic transformation of the models, a linear regression was performed to obtain the initial estimators of the parameters. The models were linearized as follows:

- Potential model: $\mathrm{LOG}(F) = \mathrm{LOG}(A) + C \times \mathrm{LOG}(X)$, giving the initial estimation of A and C.
- Maxwell model: $\mathrm{LOG}(F/X) = \mathrm{LOG}(A) - K \times X$, $K = 1/T \times r$, giving the initial estimation of A and T.
- Nonlinear Maxwell model: The initial estimators were those obtained by the Maxwell model, the initial estimation of C = 1 (linear behavior).

Then, based on these estimations, the final estimators of the models were obtained by the ap-

Table II Potential Model, Maxwell Model, and Modified Maxwell Model Fitting to the Yarns in Table I

	Model R^2 adj (%)					
Ref.	Potential	Maxwell	N/L Maxwell	Elastic Modulus A (Standard Error)	Linearization Factor C (Standard Error)	Relaxation Time T (Standard Error)
T12	97.16	97.55	**99.84**	1.20 (0.07)	1.55 (0.04)	0.39 (0.02)
T13	97.30	98.86	**99.73**	0.92 (0.08)	1.27 (0.04)	0.68 (0.05)
T14	**99.08**	97.89	98.89	0.19 (0.03)	1.13 (0.04)	—
T15	99.05	99.48	**99.72**	2.35 (0.14)	0.89 (0.03)	0.34 (0.02)
T16	98.38	98.80	**99.62**	0.56 (0.07)	1.34 (0.05)	1.09 (0.11)
T17	**98.52**	96.63	98.23	1.67 (0.16)	0.79 (0.04)	—
T18	99.21	99.30	**99.76**	2.25 (0.11)	0.85 (0.03)	0.29 (0.02)
T19	98.19	99.74	**99.96**	1.70 (0.05)	1.12 (0.01)	0.38 (0.01)
T20	97.07	99.47	**99.71**	1.49 (0.10)	1.11 (0.03)	0.39 (0.02)
T21	99.28	99.40	**99.46**	0.45 (0.05)	0.95 (0.06)	0.72 (0.16)
U12	98.61	96.94	**99.73**	0.04 (0.01)	2.43 (0.10)	8.22 (1.58)
U13	98.46	99.39	**99.95**	0.71 (0.03)	1.25 (0.02)	0.81 (0.03)
U14	99.44	98.96	**99.46**	0.56 (0.04)	0.86 (0.02)	210.0 (0.00)
U15	98.21	97.69	**99.68**	0.21 (0.03)	1.52 (0.05)	3.05 (0.42)
U16	98.70	98.77	**99.66**	0.45 (0.06)	1.36 (0.06)	1.51 (0.17)
U17	**99.30**	98.83	99.19	0.99 (0.09)	0.93 (0.03)	—
U18	98.12	98.72	**99.60**	0.62 (0.08)	1.29 (0.05)	1.10 (0.12)
U19	98.06	99.48	**99.89**	1.50 (0.06)	1.18 (0.03)	0.37 (0.01)
U20	99.42	99.65	**99.66**	1.07 (0.10)	1.03 (0.05)	0.73 (0.09)
U21	**99.43**	98.53	99.39	0.75 (0.04)	0.78 (0.02)	—

The best values of R^2 adj and the model coefficients of the best fit are shown in bold figures. The standard errors of the coefficients are shown in the parentheses.

Table III Variation of the Elastic Modulus and the Linearity Factor Across the Different Models

	Elastic Modulus A			Linearity Factor C		
Ref.	Potential	Maxwell	N/L Maxwell	Potential	Maxwell	N/L Maxwell
T12	2.04	2.11	1.20	0.96	1	1.55
T13	1.88	1.56	0.92	0.80	1	1.27
T14	0.19	0.26	0.24	1.13	1	1.03
T15	3.03	1.95	2.35	0.66	1	0.89
T16	1.10	1.07	0.56	0.94	1	1.34
T17	1.67	1.17	1.81	0.79	1	0.76
T18	2.69	1.78	2.25	0.65	1	0.85
T19	2.69	2.08	1.70	0.73	1	1.12
T20	2.57	1.84	1.49	0.69	1	1.11
T21	0.53	0.42	0.45	0.81	1	0.95
U12	0.14	0.45	0.04	1.68	1	2.43
U13	1.40	1.15	0.71	0.84	1	1.25
U14	0.56	0.45	0.56	0.86	1	0.86
U15	0.68	0.59	0.21	1.00	1	1.52
U16	0.93	0.89	0.45	0.96	1	1.36
U17	0.99	0.86	1.01	0.93	1	0.92
U18	1.32	1.05	0.62	0.87	1	1.29
U19	2.31	1.95	1.50	0.77	1	1.18
U20	1.32	1.11	1.07	0.86	1	1.03
U21	0.75	0.54	0.77	0.78	1	0.77

plication of the iterative nonlinear regression procedure.[12] The best model was selected in all cases using the maximum so-called adjusted R^2 according to the criterion of Draper and Smith.[13] The R^2 adj is the determination coefficient of the model R^2 balanced by the degrees of freedom of the fitting: R^2 adj $= 1 - (1 - R^2) \times [(n = 1)/(n = p)]$, n being the number of experimental points used for model fitting, and p, the number of the parameters of the model.

RESULTS

Table II gives the values of R^2 adj for the three models, the values of the elastic modulus A, the linearity factor C, and the relaxation time T of the best model (maximum R^2 adj) for each reference. Table III shows how much the elastic modulus A and the linearization factor C vary across the different models. The Maxwell model is able to explain the linear viscoelastic behavior. Then, its linearity factor can be considered as unity. In that case, the estimated elastic modulus A is the pure elastic modulus remaining constant along the deformation process. When linearity factors differ from unity (nonlinear viscoelastic behavior explained by the potential model and the N/L Maxwell model), the elastic modulus shows a variation along the deformation process. Consequently, the estimated elastic modulus A will be an "average" of the elastic modulus spectrum that will be different from the elastic modulus estimated by the Maxwell model.

It can be observed in Table III that when linearity factors C of the models are similar then the estimated elastic modulus A results are also very similar. For linearity factors close to unity, the estimation of the elastic modulus A was very close to that of the Maxwell model.

Figure 4 shows some fits corresponding to cotton, polyester, and acrylic yarns. Graphs (a) and (b) correspond to references T12 and U12 (cotton yarns), graphs (c) and (d) correspond to references T19 and U19 (polyester continuous filament yarns), and graphs (e) and (f) to references T14 and U14 (acrylic yarns).

DISCUSSION

By using the nonlinear Maxwell model, it is possible to account for the stress–strain behavior of the staple fiber yarns. The linearity coefficient C

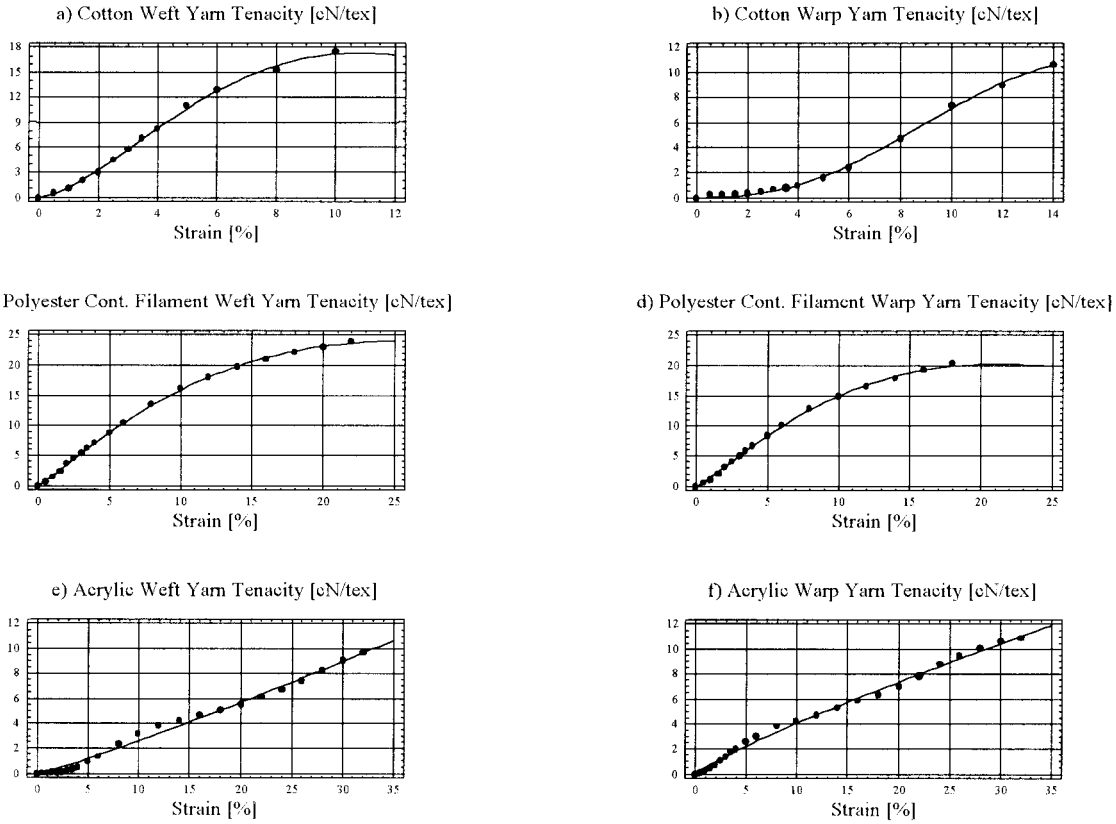

Figure 4 Stress–strain curve fits using nonlinear modified Maxwell model and potential model for (a,b) cotton, (c,d) polyester continuous filament, and (e,f) acrylic fiber yarns.

is related to the degree of disarrangement of the yarn structure in such a way that it grows with the disarrangement of the fibers into the yarn. This can be seen for the polyester yarns, where the staple yarns displayed a higher C value than that of the filament yarns. The relaxation time is related to the slippage speed between fibers and is, therefore, a parameter that can be related to the structure of the fiber composition and yarn structure.

The application of the discrimination analysis technique shows that the coefficients of the best model allow the classification of yarns in accordance with their composition. Figure 5 shows that the highest linearity factors correspond to the cotton yarns; the intermediate values, to the polyester yarns; and the lowest values, to the acrylic yarns. The values of the elastic modulus for the acrylic and cotton yarns range between 0 and 1, whereas the values for the polyester yarns are

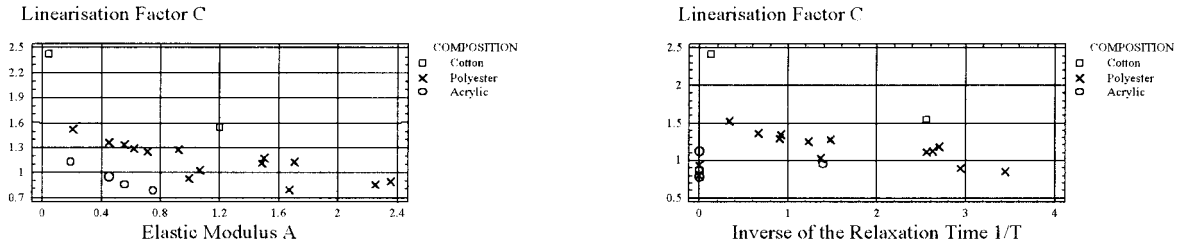

Figure 5 Distribution of the model coefficients according to the composition. The four points lying on the straight line $1/T = 0$ correspond to the potential fitting.

higher than 2. As regards the relaxation time, it may be observed that the potential model, when no slippage between fibers occurs, is applied only to two acrylic and two polyester continuous filament yarns. It may also be observed that, although the potential model is the best for four yarns (T14, T17, U14, U21), their R^2 adj's were the lowest (99.08, 98.52, 99.30, 99.43). This suggest that small deviations from the experimental points to the fitted stress–strain curves can be observed [see Fig. 4(e)], and, consequently, the potential model has to be improved in order to obtain better modeling for these yarns.

CONCLUSIONS

Fits were made on stress–strain curves of 20 yarns obtained from 10 different fabrics. The use of simple mechanical elements such as nonlinear springs and pistons can give satisfactory fits for these stress–strain curves.

The parameters of the models can be related to the fiber composition and yarn structure. The linearity factor is related to the degree of disarrangement of the structure, and the relaxation time can define the tendency of slippage between the fibers during yarn strain.

The potential model (the limit of the nonlinear Maxwell model for infinite relaxation time) is adequate when no slippage between fibers occurs during yarn strain, while the Maxwell models are adequate when slippage occurs, the slippage speed being inversely related to the relaxation time. The elastic modulus is also related to the fiber composition and yarn.

The authors are indebted to the Spanish Government, which thorough the Program for Scientific Cooperation with Iberoamerica 1997 funded the project "New Techniques of Structural Characterisation of Textile Materials."

REFERENCES

1. Ward, I. M.; Hadley D. W. An Introduction to the Mechanical Properties of Solid Polymers; Wiley: Chichester, 1993.
2. Krausz, A. S.; Eyring, H. Deformation Kinetics; Wiley: New York, 1975.
3. Ussman, M. H.; Manich, A. M.; Gacén, J.; Maillo, J. J Text Inst, in press.
4. Manich, A. M.; Ussman, M. H.; Gacén, J.; Barella, A. In Proceedings of the International Conference Young Textile Science '95, Liberec, 1995.
5. Manich, A. M.; Ussman, M. H.; Barella, A. Text Res J, in press.
6. Gacén, J.; Maillo, J.; Manich, A. M. In Proceedings of the 17 IFVTCC Kongress (Internationalen Föderation der Vereine der Textilchemiker und Coloristen), Wien, 1996.
7. Lucas, J. M.; Manich, A. M.; Ussman, M. H. In Proceedings of the International Seminar on Textile Testing Standardisation, Guimaraes, 1997.
8. Manich, A. M.; Ussman, M. H.; Gacén, J.; Maillo, J.; Barella, A. Anal Quim Int Ed 1997, 93(2), 76–80.
9. Ussman, M. H. Ph.D. Thesis, Universidade da Beira Interior, Covilhá, 1997.
10. Vangheluwe, L. Text Res J 1992, 62, 306–308.
11. Aksan, S.; Zurek, W. J Appl Polym Sci 1975, 19, 3129–3137.
12. Statgraphics Plus for Windows, Manugistics, Inc., 2115 East Jefferson Street, Rockville, MD 20852-4999.
13. Draper, N.; Smith, H. Applied Regression Analysis; Wiley: New York, 1981; p 91.